



## MECHANICS AND MATERIALS SCIENCE

## МЕХАНІКА ТА МАТЕРІАЛОЗНАВСТВО

UDC 539.4

### ESTIMATION OF THE STRUCTURAL ELEMENTS DAMAGE BASED ON COERCITIVE FORCE MEASUREMENTS. REPORT 2. THE RESULTS OF EXPERIMENTAL INVESTIGATIONS OF COERCIMETRIC CONTROL USE FOR EVALUATION OF PARAMAGNETIC AUSTENITIC STEEL DAMAGE DEGREE UNDER MECHANICAL STRESS

Oleksii Gopkalo<sup>1</sup>; Volodymyr Nekhotiashchii<sup>2</sup>; Gennadii Bezlyudko<sup>3</sup>;  
Olena Gopkalo<sup>1</sup>; Yuriy Kurash<sup>1</sup>

<sup>1</sup>*Institute for Problems of Strength named after G. S. Pisarenko, National  
Academy of Sciences of Ukraine, Kyiv, Ukraine*

<sup>2</sup>*Institute of Electric Welding named after E. O. Paton, National Academy of  
Sciences of Ukraine, Kyiv, Ukraine*

<sup>3</sup>*LLC «Special Scientific Developments», Kharkiv, Ukraine*

**Summary.** The results of experimental investigation of the coercive force response to mechanical loading of laboratory samples made of paramagnetic (in the initial state) unstable austenitic steel AISI 304 (08X18N9) associated with structural transformations of the original austenite into deformation martensite with finite ferritic-perlite decay, which causes the change in the magnetic properties of metal from paramagnetic into ferromagnetic state are given in this paper. The experimental result of coercive forces response to different damaging effect load type such as: tension and low cycle loading at voltage amplitude control («soft» load), which causes quasistatic destruction, by implementing the initial plasticity of the metal ( $\delta$ ), and the low cycle load under control the amplitude of deformation («hard» load), which causes the destruction of fatigue, due to the origin and development to the critical values of fatigue cracks are presented. The results of experimental studies of the response of the coercive force to mechanical stresses under stresses characteristic to multi-cyclic fatigue and at the presence of stress concentrators are also presented. According to the tests results, the staging of the damage accumulation processes during the «soft» and «hard» loads: the growth of the values of the coercive force corresponds to the elastic-plastic deformation (the stage of origin of the cracks), and the decrease of their values associated with the loss of solidity of the metal in the event of the appearance of pores or cracks (stages of cracks development) is determined. Establishing the damage accumulation stage by changing the direction of the kinetic curve of the coercive force after a certain number of run cycles makes it possible to construct the curve of irreversible damage (according to French) and to evaluate the cyclic durability not according to the fatigue curve (destruction) of the metal, as adopted in engineering practice, and at the stage of cracks origin, which significantly reduces the risk of destruction. Physically substantiated method of establishing the endurance limit for austenitic unstable steel, which is based on determining the growth rate of coercive force on short bases of cyclic loading is proposed. By the magnitude of the growth rate of the coercive force, one can establish the values of the endurance limit at different durability bases. The possibility of using the structroscope to detect the most deformed zones, with the determination of the main stresses direction, and the immutability of the metal in the form of pores and cracks of fatigue, surface and sub-surface defects and cracks is shown. The limitations in the possibility of assessing the degree of metal damage in multi-cyclic fatigue, including stress concentration zones, by measurements of the coercive force values of due to the sensitivity of the device to the ratio of volumes of elastic and plastic-deformed

metal in the zone of destruction (measurement) are defined. The use of the coercimetric control allows by means of the results of measuring the changes in the coercive force in the most loaded structures sections during their operation to assess the level of damage received.

**Key words:** structurescopel, coercive force, load, damage, stresses, deformation, fracture.

[https://doi.org/10.33108/visnyk\\_tntu2019.02.007](https://doi.org/10.33108/visnyk_tntu2019.02.007)

Received 18.04.2019

**Coercive force response to low-cycle «hard» load.** In this section, experimental data of the coercive force response ( $H_c$ ) to the low-cycle «hard» load of austenitic steel (under the deformation amplitude control) without affecting the damage from the cyclic creep at the stages of cracks origin and development in the symmetrical load cycle  $R_\varepsilon = -1$  are given.

It was noted in paper [1] that under the conditions of small-cycle «hard» load there is the characteristic fracture of the kinetics curve of coercivity force starting from a certain number of load cycles indicating the change in the prevailing type of accumulated damages. The kinetics of change in the values of the coercive force ( $H_c$ ), depending on the number of load cycles ( $n$ ) with the amplitude of the alternating deformation  $\varepsilon_a = \pm 0,5\%$  is shown in Fig. 1. Here the values of  $H_c$  were determined by sensors with different measuring base D65 (65 mm), D27 (27 mm) and D12 (12 mm), while orienting the sensor magnet poles along (relatively to the sample axis) the sample surface made of the tube.

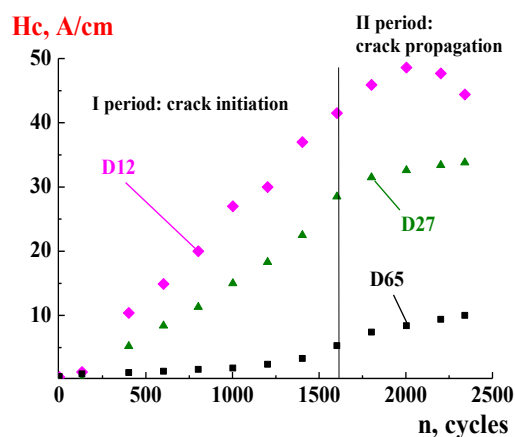


**Figure 1.** The kinetics of the coercive force values depending on the number of load cycles

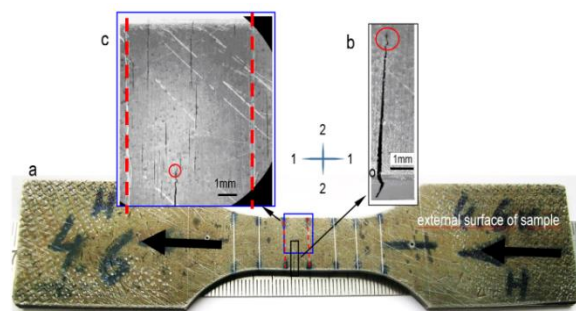


**Figure 2.** Macro images of the sample (a) after cyclic operating time before the occurrence of the main crack with the area 19% of the nominal cross-section; where b, c are the fragments of the section with cracks on the outer surface of the sample; orientation directions of the magnet poles along (1–1) and transverse (2–2) of the sample axis

The occurrence of fatigue cracks (loss of the metal solidity) in the destruction zone after 1600 cycles of cyclic fluctuating deformation resulted in the breaking point of the coercive force curve. The fracture presence on the coercive force kinetics curve, depending on the cycles of low-cycle «hard» load, indicates the presence of staged accumulation processes of metal damage. Macroscopic images of the sample after cyclic operating time up to the occurrence of the main crack with the area 19% of the nominal cross-section (a) are shown in Fig. 2. In such a case, in addition to the main crack (b), small (~ 1 mm) nonthrough cracks (c), typical only for

the outer sample surface (and, accordingly, for the pipe) and absent on the inner surface, were found in the fracture zone on the outer sample surface. This kind of fracture is due to the difference in technological residual stresses of tension and compression in the outer and inner layers of the pipe with longitudinal weld joint made of sheet metal.

The use of a stroboscope with small-sized shallow magnetization sensor (D12) with measuring base 12x12 mm makes it possible to scan with step 6 mm the sample working element surface from the pipe and to construct the distribution of the values on the outer and inner surfaces during the tests. The distribution of the coercive force  $H_c$  values on the external (*a*) and the internal (*b*) surface of the sample working length from the pipe at the low-cycle «hard» load with the elastic-plastic deformation amplitude  $\varepsilon_a = \pm 0,5\%$  in the sensor magnet poles orientation along the sample is shown in Fig. 3. Reducing the coercive force values in the fracture zone on the inner sample surface when visible cracks are absent indicates the possibility coercimetric control application for subsurface cracks detection.

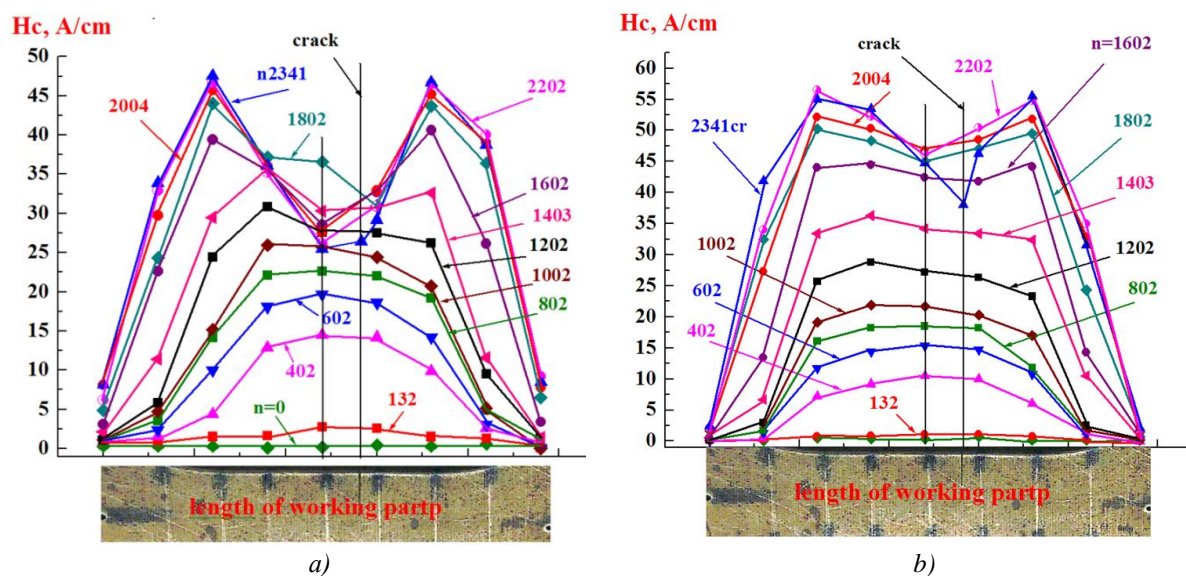


**Figure 3.** The distribution of the coercive force values  $N_c$  on the external (*a*) and internal (*b*) surface of the sample working length from the pipe at the low cycle «hard» load when orienting the sensor magnet poles along the sample

In order to study the reasons of the decrease of coercive force values in the fracture zone under low-cycle «hard» load, the measurements of the fraction (%) distribution of the ferromagnetic phase ( $\alpha$ -Fe) along the sample working length after fracture were carried out. Data concerning the fraction (%) distribution of the ferromagnetic phase ( $\alpha$ -Fe) and the coercive force  $H_c$  along the sample working length after the low-cycle «hard» load to the fracture with the elastic-plastic deformation amplitude  $\varepsilon_a = \pm 0,5\%$  are presented in Fig. 4.

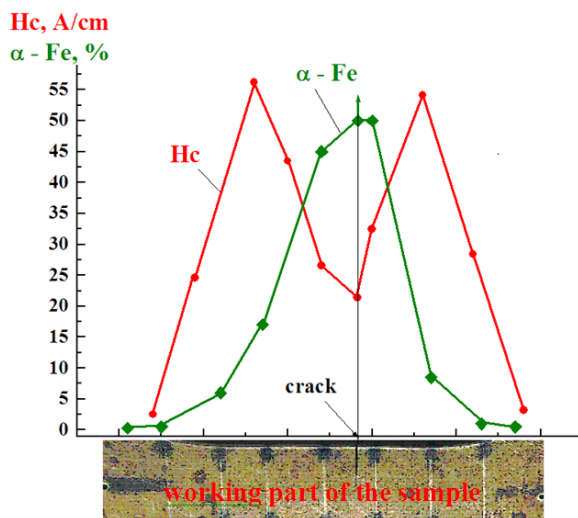


**Figure 4.** The distribution of the ferromagnetic phase ( $\alpha$ -Fe) volume and the coercive force  $H_c$  along the sample working length after the low cycle load till fracture

It follows from the obtained data that the decrease in the coercive force values in the area adjacent to the fracture zone is associated with the loss of material solidity (the appearance and development of fatigue cracks). In this case, the loss of metal solidity does not affect the ferromagnetic phase ( $\alpha$ -Fe) fraction growth due to the continuous metal elastic-plastic deformation including that between the cracks. Loss of metal solidity causes more intense decrease in magnetic properties, including coercive force, than elastic-plastic deformation contributing to the increase of ferromagnetic phase ( $\alpha$ -Fe) volume even with defects (cracks).

The microstructure of the sample metal, respectively, in the fracture zone (the central part of the sample working part) (a) and on its working part periphery (near the fillet) (b) is presented in Fig. 5 a, b. The decrease of the coercive force values working part from ( $H_c$ ) 3 55 A/s/m on the sample working part periphery to 20 A/s/m in the fracture zone (see Figures 3 a, b) is due to the metal solidity loss with the occurrence of fatigue cracks and accumulation of other damage (for example, the formation of pores) of metal in the fracture zone.

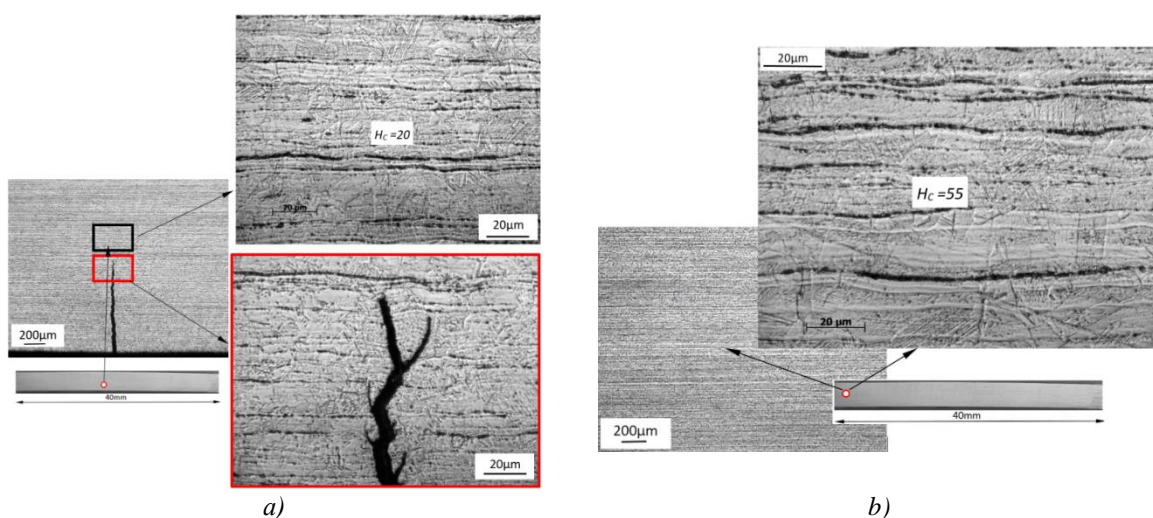


**Figure 5.** Microstructure of the sample metal in the fracture zone (a), where  $H_c = 20$  A/cm and at the periphery of its working part (b), where  $H_c = 55$  A/cm



More distinctly, the kinetics of the change in the coercive force of low-cycle «hard» load becomes obvious in the fracture zone while using structuroscope with reduced base of D12 sensor for measuring the coercive force values. The kinetics of the coercive force on the outer and inner surfaces of the sample from the pipe in the fracture zone at the position of the sensor magnet poles along the sample working length at low-cycle «hard» load with the deformation amplitude  $\varepsilon_a = \pm 0,5\%$  is shown in Fig. 6.

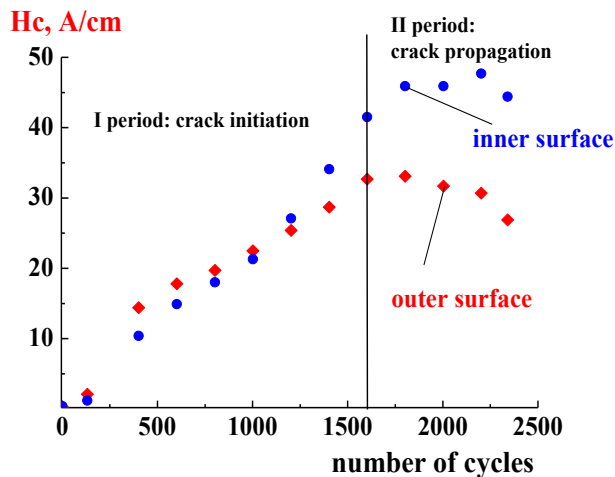


**Figure 6.** The kinetics of the coercive force on the outer and inner surface of the sample from the pipe in the fracture zone

The occurrence of fatigue cracks (loss of metal solidity) on the outer surface of the sample from the pipe results in the reduction in the coercive force values, while the internal surface, where plastic deformation continues and fatigue cracks are absent,  $H_c$  growth continues with the following gradual decrease of these quantities. The increase in the coercive force values corresponds to the elastic-plastic deformation (the stage of cracks origin), and the decrease of  $H_c$  values – the stage of cracks development associated with the loss of metal solidity. This circumstance indicates the possibility of monitoring the damage accumulation processes both on the product surface and in the subsurface layers of the metal (over the defect) during the operation, for example, from the internal surface, which is not accessible.

Thus, under cyclic loading, the use of coercimetric control enables by the kinetics of coercive force change after a certain operating time to determine the moment of metal solidity loss and to construct the curve of irreversible damage (such as French line) and to evaluate the cyclic life not according to the fatigue curve (fracture) of the metal, as adopted in engineering practice, but at the stage of cracks, which significantly reduces the fracture risk.

For conditions of low cycle «hard» loading the dependence of the coercive force values of coercive on the orientation of the sensor magnet poles relatively to the direction of loading was determined experimentally. It makes it possible for real constructions to determine the direction of the main stresses and to detect the occurrence of surface and subsurface fatigue cracks. Data of the coercive force values in the crack zone and in the adjacent areas after the cyclic operating time (with the deformation amplitude  $\varepsilon_a = \pm 0,4\%$ ) to the number of cycles  $n = 7204$  and  $n = 7328$  (with the area of the crack being 16.7% and 33.4% respectively nominal) are shown in Fig. 7.

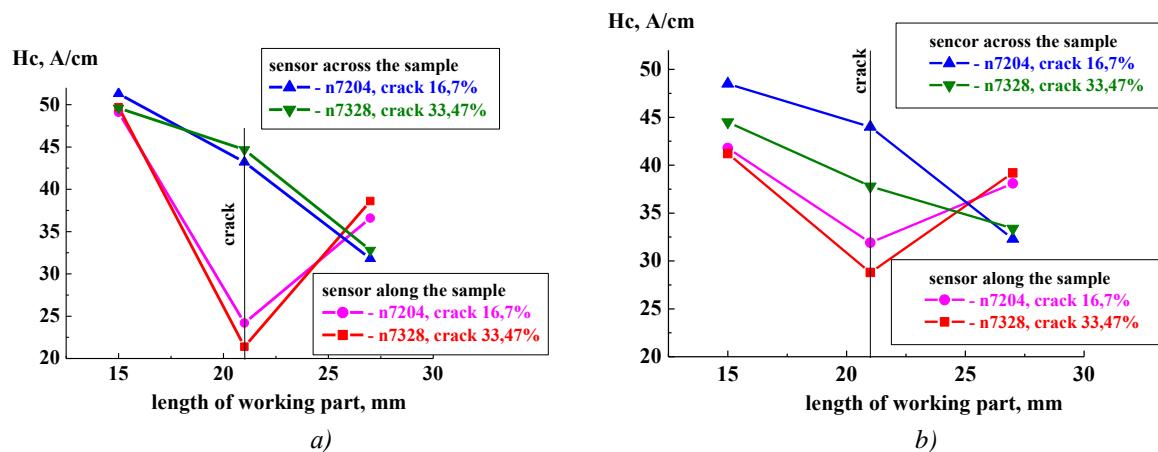


**Figure 7.** The coercive force value on the external (a) and internal (b) surface of the sample when orienting the sensor magnet poles along and across the sample working part (at  $n = 7204$  and  $n = 7328$  the number of cycles)

Measurement of the coercive force values was carried out at the location of the fatigue crack in the middle between the sensor magnet poles and on the distance of the sensor center 6 mm in both directions from the crack (in adjacent to the crack sections) from the outer (a) and inner (b) sample surfaces while orientating the sensor magnet poles along and across its working part. When orienting the sensor magnet poles along the outer surface of the sample working part (along the applied load direction, that is, perpendicular to the crack direction), in the crack area there are lower coercive force values relatively to the peripheral zones, contributing to their detection. It should be noted that when orienting the sensor magnet poles along the sample working part on the inner surface of the sample from the pipe, where there are no fatigue cracks, there is also coercive force values decrease (Fig. 7 b). This confirms the possibility of detecting the subsurface cracks by means short-base sensor D12.

**Coercive force response to the samples low-cycle «soft» load without stress concentrators.** This section deals with the experimental data on the coercive force response to the low-cycle «soft» load (without the effect of fatigue damage) under static and cyclic tension, when the processes of damage accumulation under these conditions are identical.

The diagrams of static and cyclic tension and the change in the coercive force values, measured by the D65 sensor, at tension (a) and the coercive force dependence  $H_c$  on deformations  $\varepsilon$  (b) under stepped stretching with unloading, at loaded and unloaded state are shown in Fig. 8. It should be noted that at the initial stretch stage, including the elastic-plastic area, changes in the coercive force values the occur in accordance with the tensile diagram. With further plastic deformation, there is some lagging in the growth rate of the coercive force values relatively to the applied stresses. When the values of accumulated deformations  $\sim 30 \dots 35\%$  are reached there is a sharp decrease in the coercive force values. The regularities of sharp decrease in the coercive force values after reaching the extremum at tension are similar to the «hard» load, probably connected with the loss of metal solidity through the formation and growth of pores number and size. According to the literature sources [2] one of the reasons for such coercive force behavior is the reduction of residual compressive stresses due to the metal density decrease caused by the accumulation of crystals damages, the formation of pores and inconstancies in plastic deformation by tension.

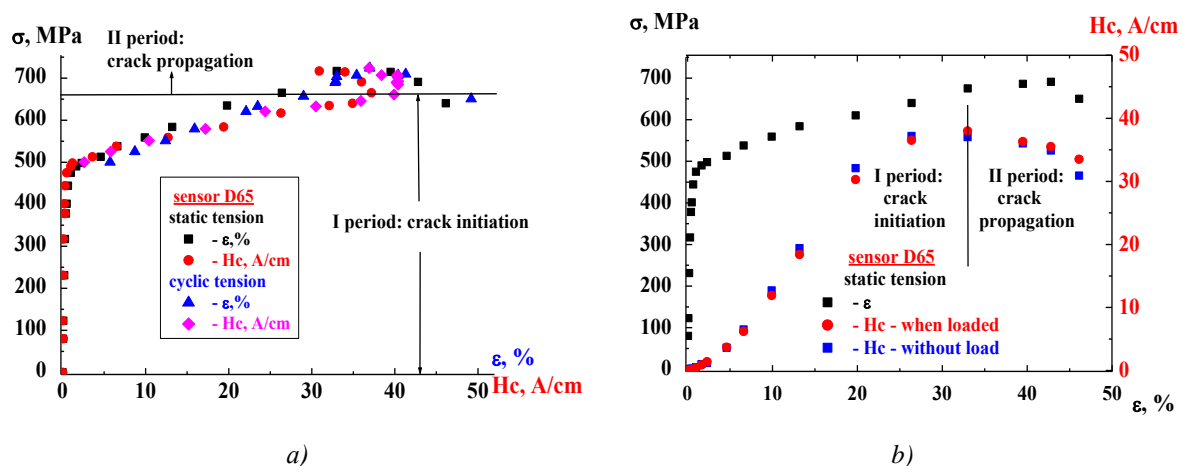


**Figure 8.** Diagrams of static and cyclic tension (a) and the dependence of the coercive force  $H_c$ , measured by the D65 sensor on strain (b) during tension with unloading in loaded and unloaded state

It should be noted that the coercive force value during the stepped tension with unloading in the loaded and unloaded state, practically, coincide. Thus, according to the size of the coercive force on the ascending or descending curves areas, the residual metal strength can be estimated at different damage stages irrespectively to the load availability.

The tensile diagram and the dependence of the coercive force values  $H_c$  measured by D27 sensor and the fraction of the ferromagnetic phase ( $\alpha$ -Fe) on the deformations ( $\epsilon$ ) under laboratory samples tension is presented in Fig. 9. It should be noted that under stepped increase of tensile deformation on 5% the growth of the coercive force values is observed only when the deformation reaches  $\sim 25\%$  (at stresses below the metal strength limit), and with further deformation there is a sharp decrease of  $H_c$  values. At the initial loading stages, the growth rate of the coercive force  $H_c$  is much more sensible to the deformation change than to the occurrence of the ferromagnetic phases (ferrite and martensite deformation) in the austenitic matrix, and when it reaches the limiting deformations ( $\epsilon \geq 40\%$ ) it takes the avalanche-like character.

The use of structurescope with the reduced base of D12 sensor made it possible to investigate the distribution of the coercive force values along the length of the sample working part under tension and to construct the  $H_c$  kinetics in the sample local surface areas. The distribution of accumulated deformations  $\epsilon_n$  and the coercive force  $H_c$  along the working length of the sample from the pipe with stepped increase in tensile deformation by 5% is shown in Fig. 10. At tension up to the level of nominal deformation  $\sim 25\%$  in the most deformed sample zone the increase in the coercive force up to 67,0 A/cm occurs, and with further loading, there is the decrease in  $H_c$  values to 15,3 A/cm with gradual loss of the metal solidity in the fracture zone.

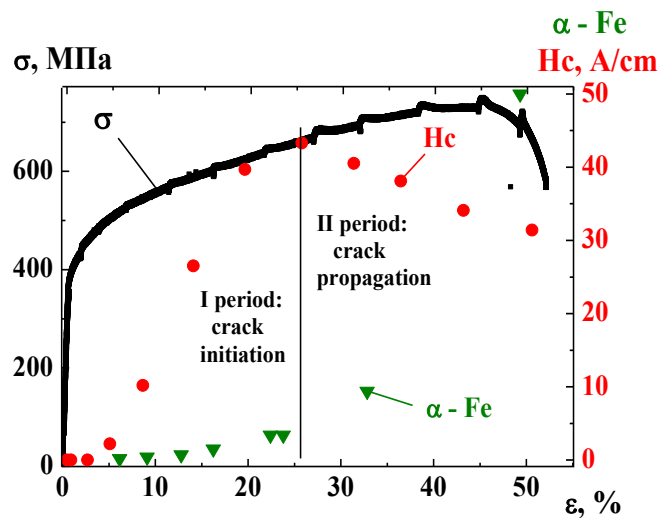


**Figure 9.** The tension diagram ( $\sigma - \varepsilon$ ) and dependence of the coercive force  $H_c$  and the ferromagnetic phase ( $\alpha$ -Fe) fraction on the deformations ( $\varepsilon$ ) under static tension of the laboratory samples

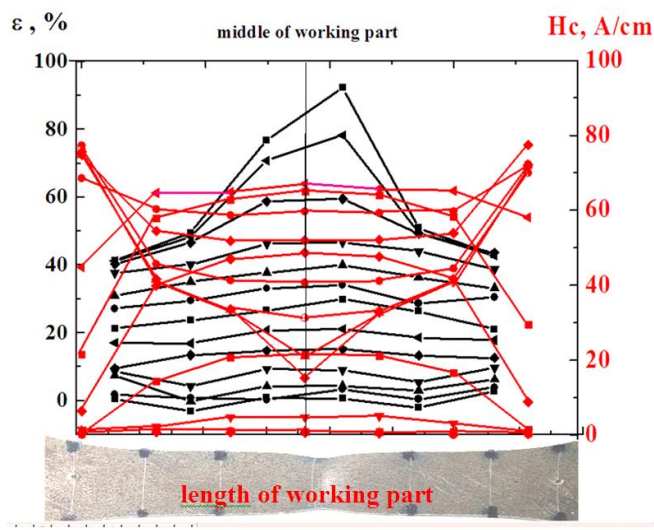


**Figure 10.** The distribution of deformations  $\varepsilon$  (black lines) and the coercive force  $H_c$  (red lines), measured by means of D12 sensor, along the length of the sample working part under tension

The dependence of the coercive force values measured by means of D12 and D27 sensors on the accumulated deformations ( $\varepsilon$ ) in the most deformed local zone (fracture) of the sample under tension during orientation of the sensor magnet poles along and across the outer surface of the working part of the sample from the pipe is shown in Fig. 11. While orienting the sensor magnet poles in the longitudinal direction of the sample working part of the, the maximum values of the coercive force are 13% greater than the similar values when orienting the sensor magnet poles in its transverse direction. The presence of ascending and descending areas on the graphs can indicate the stages and changes in the prevailing mechanisms of damage accumulation in the metal during tension. The ascending curve area corresponds to elastic-plastic deformation (the stage of cracks origin), and the descending – the formation and development of pores and cracks (the stage of cracks development).



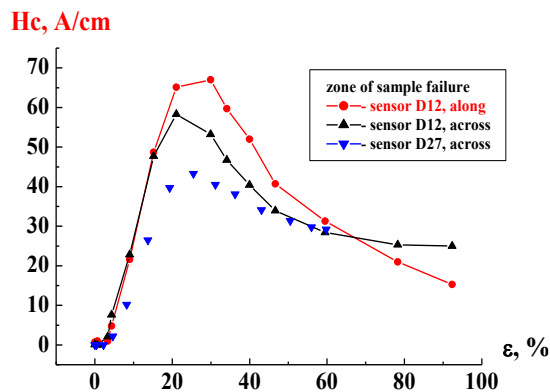


**Figure 11.** Dependence of the coercive force values measured by means of D12 and D27 sensors from the accumulated deformation ( $\varepsilon$ ) in the most deformed local zone (fracture) of the sample under tension while orienting the sensor magnet poles along and across the outer surface of the working part of the sample from the pipe

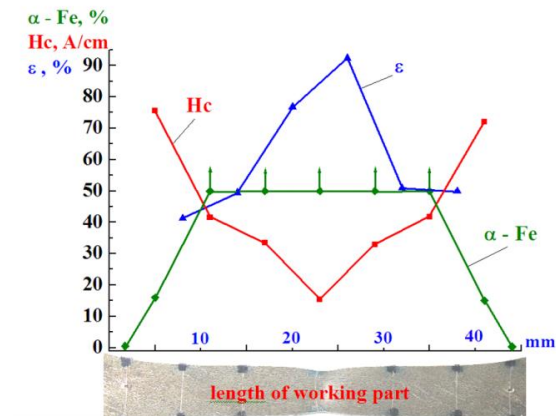


**Figure 12.** Distribution of the ferromagnetic phase ( $\alpha$ -Fe) fraction, the coercive force  $H_c$ , and accumulated deformations  $\varepsilon$  along the sample working length after fracture under tension

Thus by the coercive force value  $H_c$  in the ascending or descending curve sections, one can estimate the residual metal strength under tension. When monitoring the technical condition of structural elements taking into account the orientation of the sensor magnet poles relatively to the investigated surface, the most deformed zones and the main stresses direction can be determined.

Data concerning the distribution of the fraction (%) of the ferromagnetic phase ( $\alpha$ -Fe), the coercive force  $H_c$  and the accumulated deformations ( $\varepsilon$ ) along the length of the sample working part after the fracture under tension are shown in Fig. 12. The above given data confirm that with deformation accumulation of more than 25% (in this case after the fracture the accumulated deformation in all investigated areas of the sample working part exceeds 40%) there is decrease in the coercive force values, which is probably due to the loss of metal solidity. At the same time, the growth of deformations in the examined zones of the sample working part causes the increase of the fraction (%) of the ferromagnetic phase ( $\alpha$ -Fe) irrespectively of the loss of material solidity. The increase in the fraction (%) of the ferromagnetic phase ( $\alpha$ -Fe) should result in the increase of the coercive force values, but this does not occur due to the dominant influence of the loss of metal non-solidity in the form of pores and cracks, which significantly reduces the magnetic properties of the metal and including  $H_c$  value. Unfortunately, in the sample central part, it was not possible to measure the fraction (%) of the ferromagnetic phase ( $\alpha$ -Fe) because of the restriction (50%) of the measuring range used in this work for the ferritometer «Ferritgaltmesser 1.053 Forster». Values excess ( $\alpha$ -Fe) over 50% is indicated by arrows in Fig. 12.

Investigation of microstructure in the fracture zone and in the peripheral areas showed significant differences (Fig. 13). Significant decrease in the values of coercive force ( $H_c$ ) from 75A/cm at the periphery to 15A/cm in the most deformed sample working area under deformation  $\varepsilon_H=85\%$ , preceding the fracture, can probably be explained by the pores and cracks development in the longitudinal direction (in the axial direction, which coincides with the rolling texture). Since the rolling texture of the tubular steels is characterized by elongated and grouped on separate inclusion planes, the exfoliation cracks are formed along the distribution surfaces between the elongated (during the rolling) inclusions (mainly sulfides) and the matrix (the main metal).

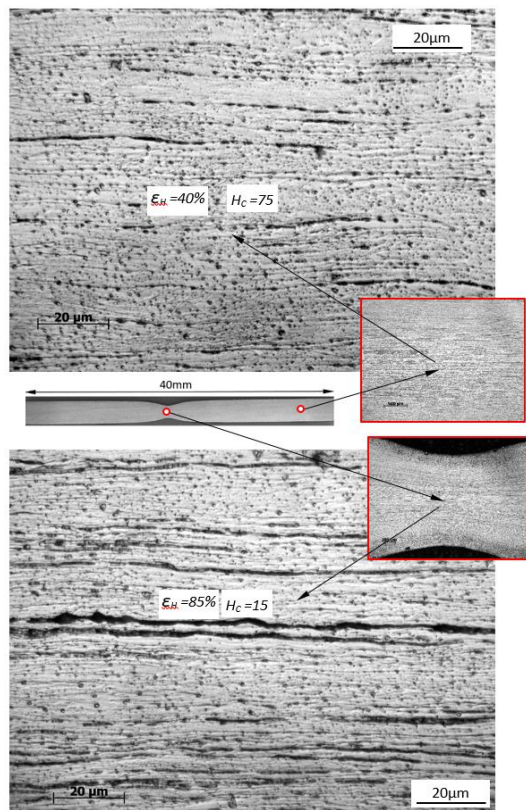


**Figure 13.** Microstructures of metal samples made of AISI 304 steel in the fracture zone and in the peripheral areas after tension up to fracture

Thus, the loss of metal solidity causes the significant decrease in the values of the coercive force (magnetic properties of the metal), despite the increase in the ferromagnetic phase ( $\alpha$ -Fe) fraction, the effect of which is leveled in comparison with the first factor.

**Coefficient response to low-cycle «soft» load of samples with stress concentrators.**

The use of the structroscope with a small dimensional D12 sensor allowed to change the orientation of the sensor relative to the direction of loading and to construct a diagram of the distribution of the values of coercive force on the surface of laboratory samples with stress concentrators under static and cyclic tension.

The tests for determination of stresses concentrators influence on the coercive force response on mechanical loadings on cycling tension of laboratory samples with through «dead» openings  $\varnothing 1,54$  mm (zone 2) and  $\varnothing 3,05$  mm (zone 4) with depth 2,2 mm (half of the sample thickness) were carried out. Measurements of the coercive force values were carried out both on the sample surface directly on the openings (side I) and on the opposite side of the sample (opposite the openings, side II). For comparison, the measurements of the coercive force values on the sample surface between the stress concentrators (zone 3) were also carried out.

The diagrams of the coercive force values distribution on the surface of the laboratory samples in the non-through («deaf») openings (side I) zone and on the opposite side (side II, opposite the openings) in cyclic stroke tests are shown in Fig. 14. As it follows from the results obtained, the coercive force value in the stress concentrators zone («deaf» openings) and the opposite side (opposite the openings), practically, coincide, despite the absence of metal in the opening cavity.

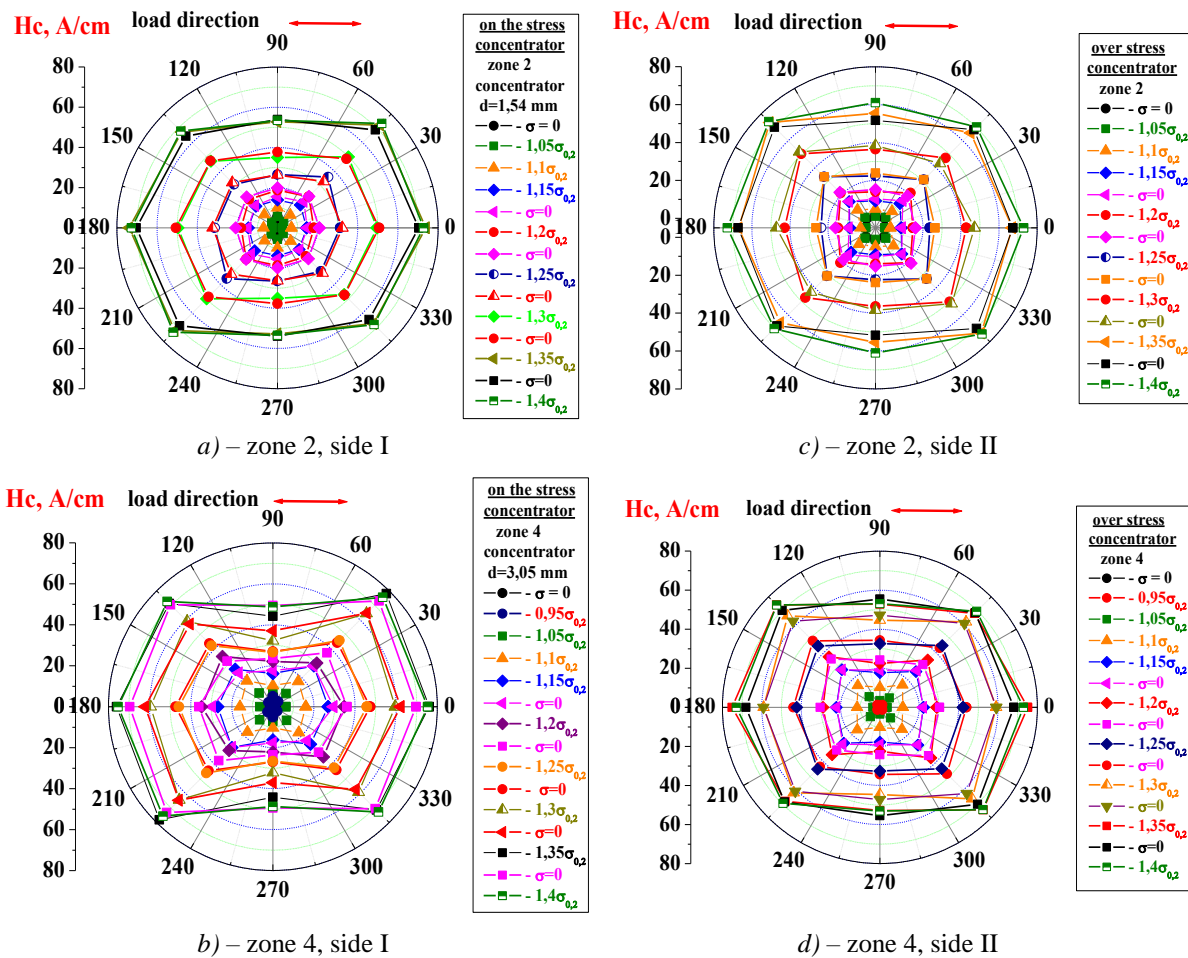


**Figure 14.** Diagrams of the coercive force values distribution on the surface of the laboratory sample with stress concentrators from non-through holes:  $\varnothing 1,54$  mm (zone 2, side I) (a) and  $\varnothing 3,05$  mm (zone 4, side I) (b) and corresponding diagrams along the sample surface on the opposite side in front of non-through through openings:  $\varnothing 1,54$  mm (zone 2, side II) (c) and  $\varnothing 3,05$  mm (zone 4, side II) (d)

For comparison, in Fig. 15 similar (see Figure 14) diagram of the coercive force values distribution on both surfaces of the laboratory sample between stress concentrators (zone 3) are given. As it follows from the results obtained, the coercive force value in zones between the stress concentrators on both sample sides, practically, also coincide.

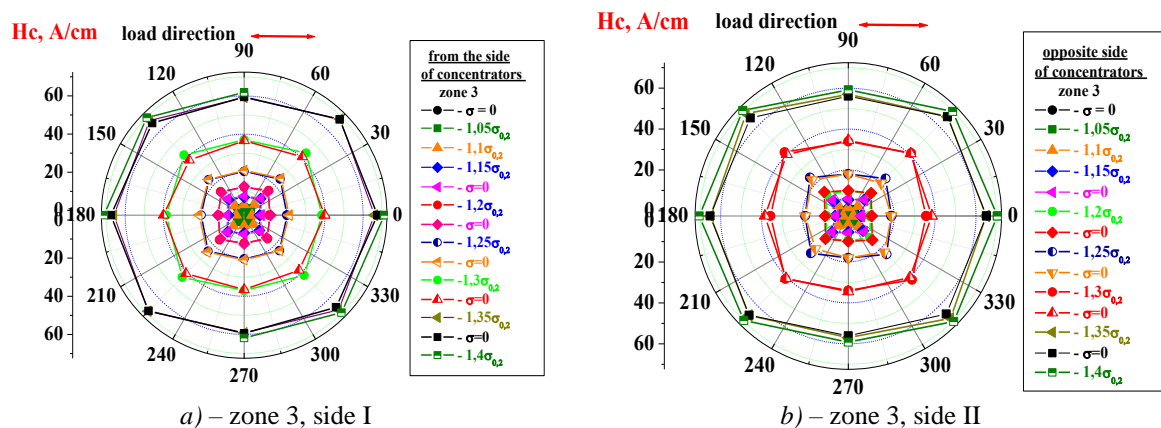


**Figure 15.** The diagrams of the coercive force values distribution on the surface of the laboratory sample between the concentrators from the holes  $\varnothing 1,54$  mm and  $\varnothing 3,05$  mm (zone 3, side I) – a) and on the opposite side (zone 3, side II) – b)

Certain differences in the diagram nature and higher (10 ... 15%) absolute coercive force values in the stress concentration zones and on the opposite side of the sample opposite the openings relatively to the zones between the concentrators are probably due to the distribution of stresses in the concentrator zone (Fig. 16). These differences are related to the sensitivity of the device to changes of the coercive force values in zones of stress concentration and are determined by the ratio of elastic-plastic deformed metal volumes in the measuring zone.

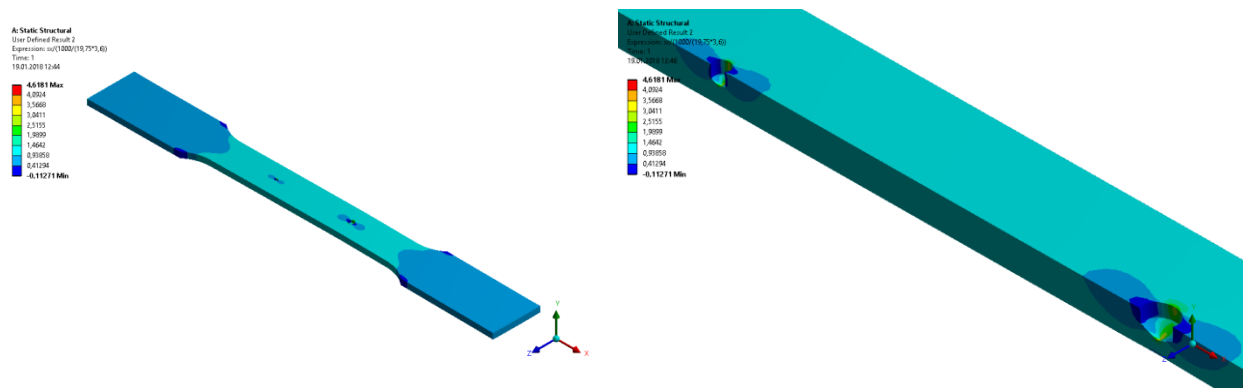


**Figure 16.** Distribution of relative axial stresses  $\frac{\sigma_x}{\sigma_{x \text{ HOM}}}$  under sample tension with non-through openings

It should be noted that the diagram nature of in the stress concentrators zones and on the opposite side of the sample in front of the openings differs by a greater anisotropy of the coercive force values in two mutually perpendicular directions (relatively to the loading direction) than in zones between stress concentrators.

Thus the obtained results of the comparison of the character of the coercive force values distribution in stress concentrator zones and on the opposite side of the sample in front of the openings and beyond their limits, did not reveal more significant differences.

**Coercive force response to multi-cycle load of samples without stress concentrators.** To determine the response of the coercive force to the multi-cycle load, tests of laboratory samples without stress concentrators with of the working part dimensions 28x14x5 mm on the axial alternating tension-compression with the frequency 80 Hz under stresses lower than fluctuation limits with stresses cycle asymmetry  $R_\sigma = -1$  were carried out.

The dependence of the coercive force on the stress amplitude in different zones (zones 1 ... 6) along the length of the sample working part is shown Fig. 17. Under cyclic loading with stress amplitude  $\sigma_a = 0,6 \sigma_{0,2}$  in the range  $0 \dots 1,5 \times 10^6$  of the cycles number, the coercive force value  $H_c$  does not practically change confirming the assumption that there is no significant change in the metal structure, and the value of cyclic stress amplitude can correspond to the endurance limit. The increase in the stress amplitude with 3% step causes the growth in the coercive force values due to the metal structure change. Under cyclic loading at the rate of the coercive force growth, we can determine the values of the limited endurance limits at different durability bases. Zero value of the coercive force growth rate corresponds to the value of the endurance limit for multi-cyclic fatigue.



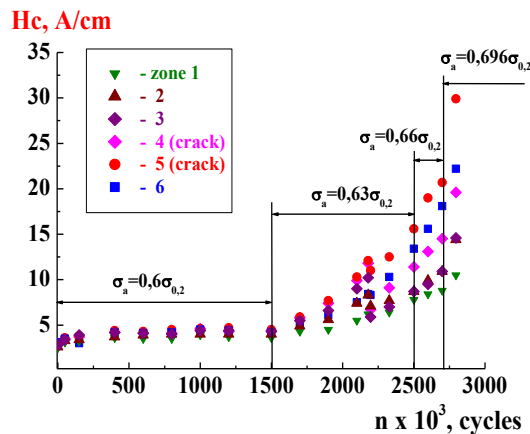


**Figure 17.** The dependence of the coercive force on the stresses amplitude in different lengths of the sample working part zones

The obtained results of laboratory samples tests on multi-cycle fatigue made it possible to change the direction of the coercive force curve, to develop simpler method for constructing the irreversible damage curve (according to French) where the limit of inverse and irreversible damage is considered to be extremum (maximum values) on the coercive force curve at a certain number of mechanical loading cycles (Fig. 18). Similar results were obtained for the same austenitic steel for the low-cycle fatigue range (see Figures 1 and 6), where it was determined that the change in the coercive force tendency to the increase or decrease of  $H_c$  values is associated with the change of the accumulated damage character [1, 3, 4].

The results of testing the scheme of construction of the irreversible damage curve based on the data of the coercive force kinetics (Fig. 18) under mechanical load in the range of multi-cycle fatigue are shown in Fig. 19. In order to verify the scheme of the irreversible damage curve construction, the preliminary cyclic operating time of 5 samples with stresses amplitude  $0,75 \sigma_{0,2}$  to the number of cycles  $n = 1 \times 10^4$ ,  $3 \times 10^4$ ,  $4 \times 10^4$ ,  $5 \times 10^4$  and  $5,5 \times 10^4$  cycles with the following loading with lower stresses amplitude  $0,6 \sigma_{0,2}$  up to  $n = 1 \times 10^6$  cycles (samples #1 ... #4), or to fracture (sample #5). On the basis of the obtained data the line of irreversible damage was constructed.

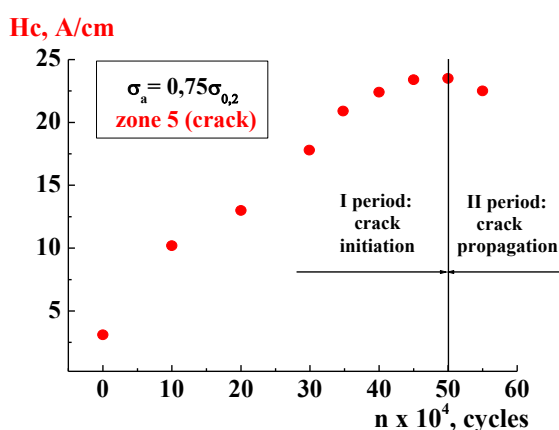


**Figure 18.** The kinetics of the coercive force change  $H_c$  from the number of load cycles  $n$  at frequency 80 Hz in the fracture zone of the laboratory sample working part at the stresses amplitude  $\sigma_a = 0,75 \sigma_{0,2}$

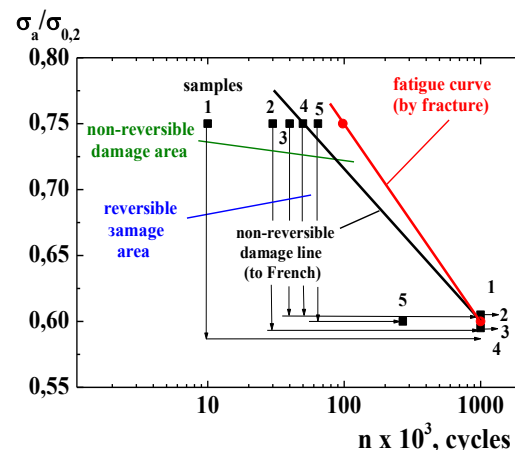


**Figure 19.** Scheme of the irreversible damage curve construction (by French): sample 1 – operating time  $n = 1 \times 10^4$  cycles,  $H_c = 10,3$  A/cm;  
2 –  $n = 3 \times 10^4$  cycles,  $H_c = 17,8$  A/cm;  
3 –  $n = 4 \times 10^4$  cycles,  $H_c = 22,4$  A/cm;  
4 –  $n = 5 \times 10^4$  cycles,  $H_c = 23,5$  A/cm;  
5 –  $n = 5,5 \times 10^4$  cycles,  $H_c = 22,4$  A/cm

In fig. 20 shows The kinetics of the coercive force change in different in lengths zones of the laboratory sample working part under the stress amplitude  $\sigma_a = 0,75 \sigma_{0,2}$ . It should be noted that in the range of cyclic operating time  $n = (50 \dots 55) \times 10^4$  cycles after reaching the maximum value there is the change in the coercive force change trend from the increase to the decrease in the fracture zone and adjacent to it areas. When scanning the sample surface with the step 6 mm (half of the base  $12 \times 12$  mm of the coercive force measurement sensor), the fracture crack was in zones 4 and 5. Zones 1 (near passive capture) and zone 6 (near active capture) are located partly on the fillets and edges of the laboratory sample working part (the working part of the coercive force sensor for measuring overlaps the fillet part and the edge of the sample working length).

The distribution of the coercive force values along the length of the sample working part is shown in Fig. 21. It should be noted that despite the fact that during the laboratory samples production the cross-sectional area of the middle of the sample working part was deliberately lowered by  $\sim 1\%$  relatively to the peripheral zones, during fatigue tests (with the loading frequency 80 Hz), the fracture of the most laboratory samples was closer to the active capture of the test machine (in the figure on the right), where the coercive force value is 3 times greater than that of the passive capture (in the figure on the left). This circumstance confirms the assumption about the unevenness of the metal load distribution under the frequency 80 Hz on the sample working length (load and, accordingly, the metal damage, estimated by the coercive force values near the active capture larger than near the passive capture).

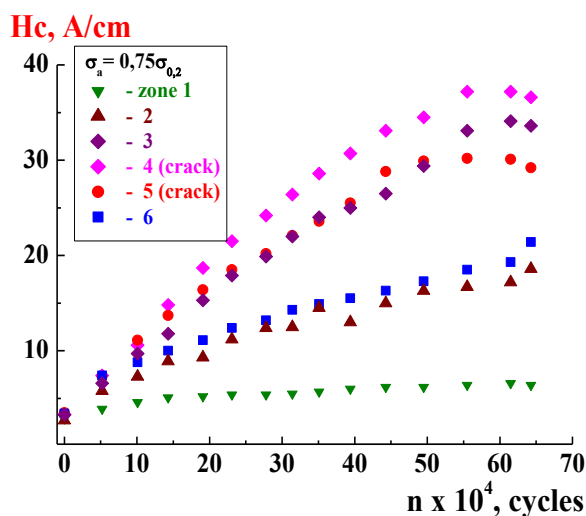


**Figure 20.** The kinetics of the coercive force change  $H_c$  in different lengths of the laboratory sample working part zones under stresses amplitude  $\sigma_a = 0,75 \sigma_{0,2}$

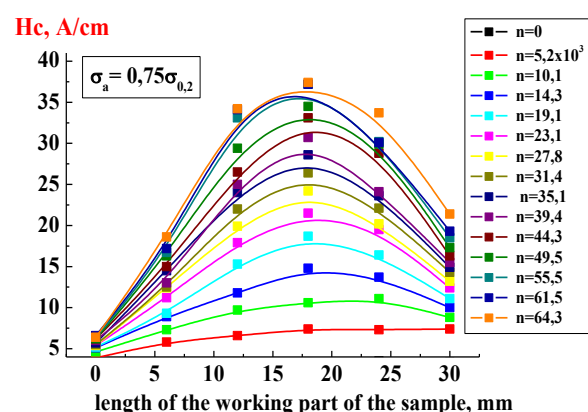


**Figure 21.** Distribution of the coercive force values along the length of the sample working part

Thus the obtained results of the tests on multi-cyclical fatigue made it possible to develop physically substantiated method for determination the endurance limit for unstable austenitic steels based on determining the growth rate of the coercive force values on short test bases ( $n = 1 \times 10^5 \dots 2 \times 10^5$  cycles number, corresponding to 20 ... 40 minutes of cyclic load at 80 Hz frequency). In addition, on the basis of the obtained data, rather simple method of the irreversible damage curve construction (according to French) for unstable austenitic steels based on the determination of the extremum (maximum) on the kinetic coercive force curve during the cyclic operating time, after which the decrease of  $H_c$  values as the result of the

irreversible damage accumulation. The use of the developed method for irreversible damage curve construction (according to French) enables steels to reduce significantly the fracture risk for unstable austenitic while evaluating the structure residual metal life.

### Coersive force response to multi-cycle load of samples with stress concentrators.

The diagrams of the coercive force values distribution along the surface of the sample with the stress concentrator in the form of a non-through (deaf) opening  $\varnothing 1,35$  (1.8 mm deep, corresponding to half thickness of the sample) in the opening area (*a*) and on the opposite to the «deaf» opening side of the sample (*b*) are shown in Fig. 22 *a, b*.

For comparison, the diagrams of the coercive force values distribution along the surfaces of two opposite sides (respectively, (*a*) and (*b*) of the continuous sample section (without concentrator) between the opening and the sample working part boundary are presented in Fig. 23.

It follows from the given data that the coercive force values in the stress concentrator zone (and symmetrically on the opposite side of the sample) is approximately 2 times greater than the similar values in the zones outside the concentrator. In this case, the coercive force values of the in the opening area is approximately 25% higher than the similar ones on the opposite side of the sample. These differences in the coercive force values within the stress concentrator zones and beyond them, are related, probably, to higher values of stresses (strains) in stress concentration zones and their distribution across the sample (see, for example, Fig. 16) and their lower values outside the concentrator and their influence on *Hc* value.

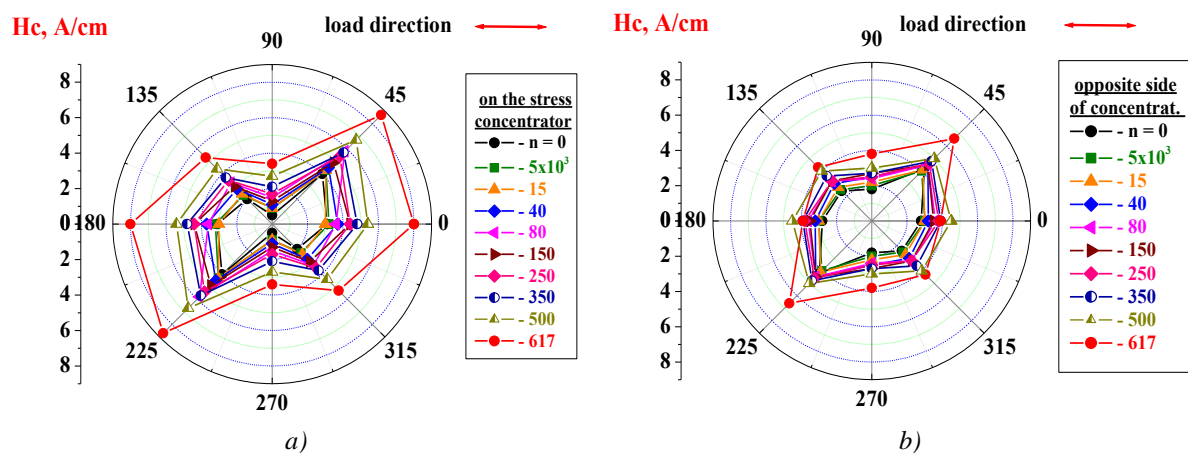


**Figure 22.** The diagrams of the coercive force values distribution along the sample surface with the stress concentrator in the opening area (*a*) and above it (*b*) (opposite to the sample opening)

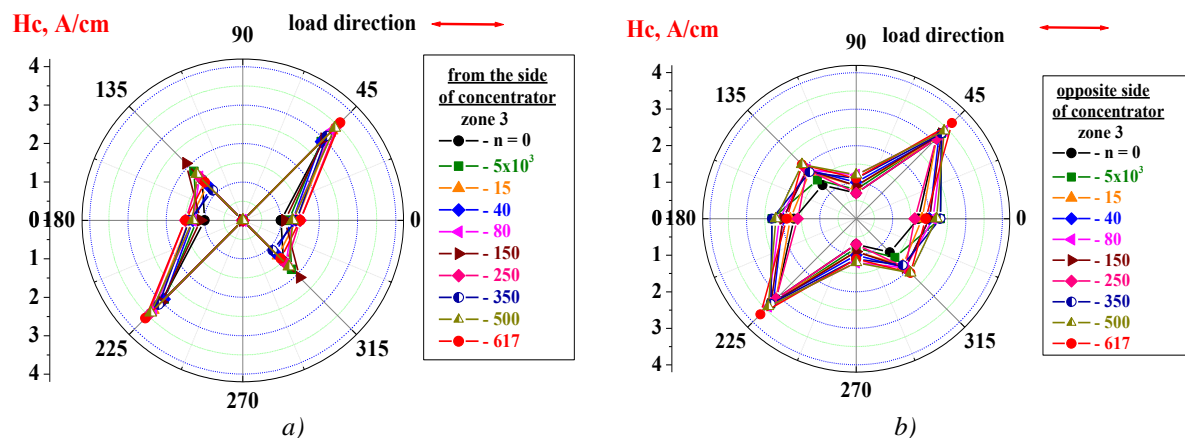


**Figure 23.** The diagrams of the coercive force values distribution along two sides of the continuous parts (without opening) between the working part edge and the opening (*a*), and on the opposite sample side (*b*)

The diagrams of the coercive force values distribution along the external (a) and internal (b) sample surfaces with the stress concentrator in the form of the weld joint (Fig. 25) are shown in Fig. 24 a, b.

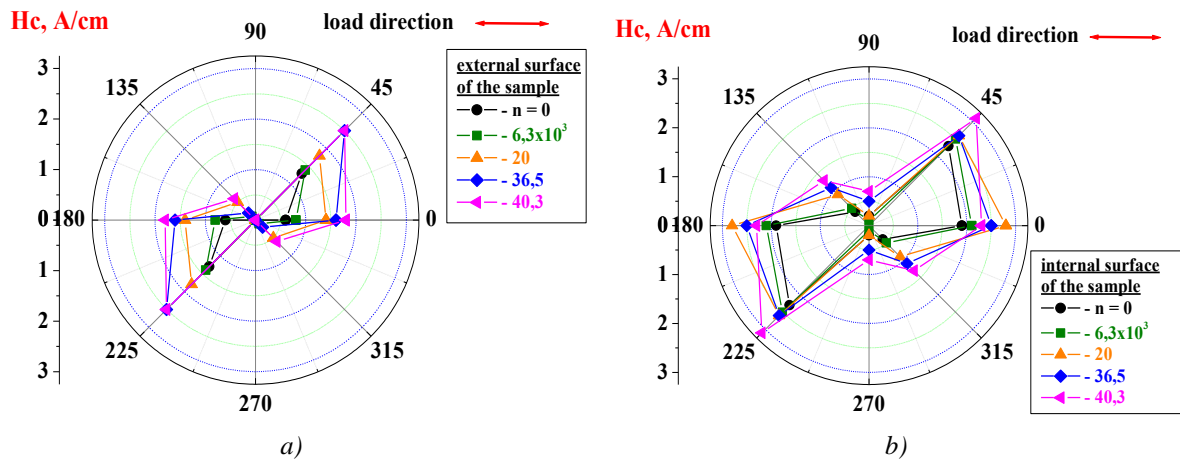


**Figure 24.** The diagrams of the coercive force values distribution along the external (a) and internal (b) sample surface with the stress concentrator in the form of the weld joint

Differences in coercive force diagrams character and their maximum values on the external and internal surfaces of the sample with the weld joint are probably due to the differences in the geometric parameters of the weld joint on the sample thickness (which in its turn affects the stress concentration degree and the stresses distribution on the sample cross section).

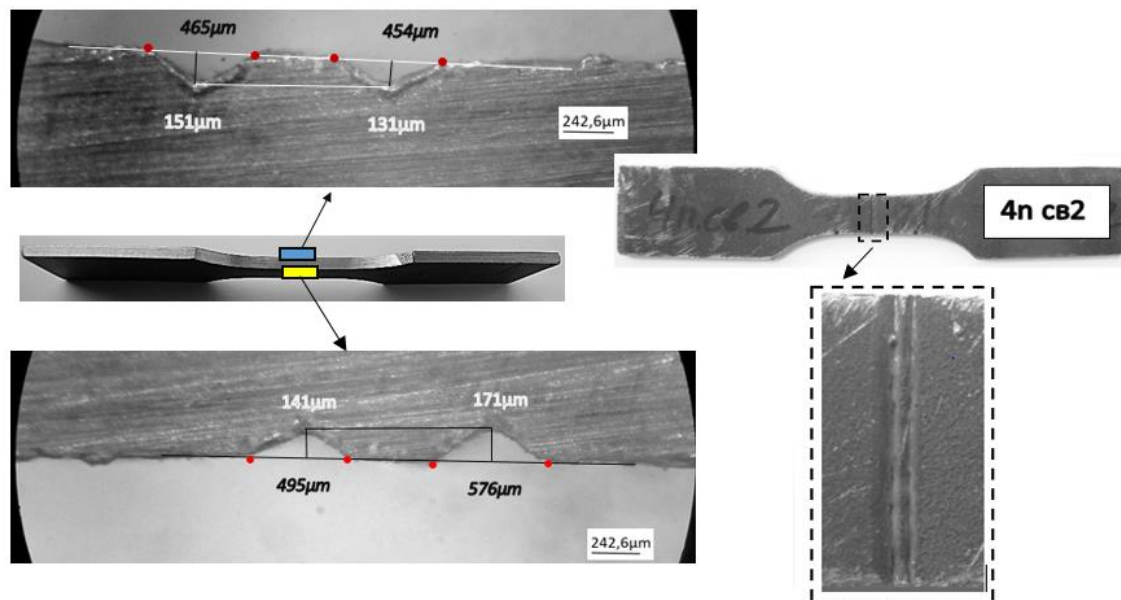


**Figure 25.** Macro images of the laboratory sample from AISI 304 steel with stress concentrator in the form of the weld joint



For comparison the diagrams of the coercive force values distribution from two opposite sides (relatively, (a) and (b)) of the continuous sample parts (without the weld joint) between the edge of the sample working part and the weld joint.

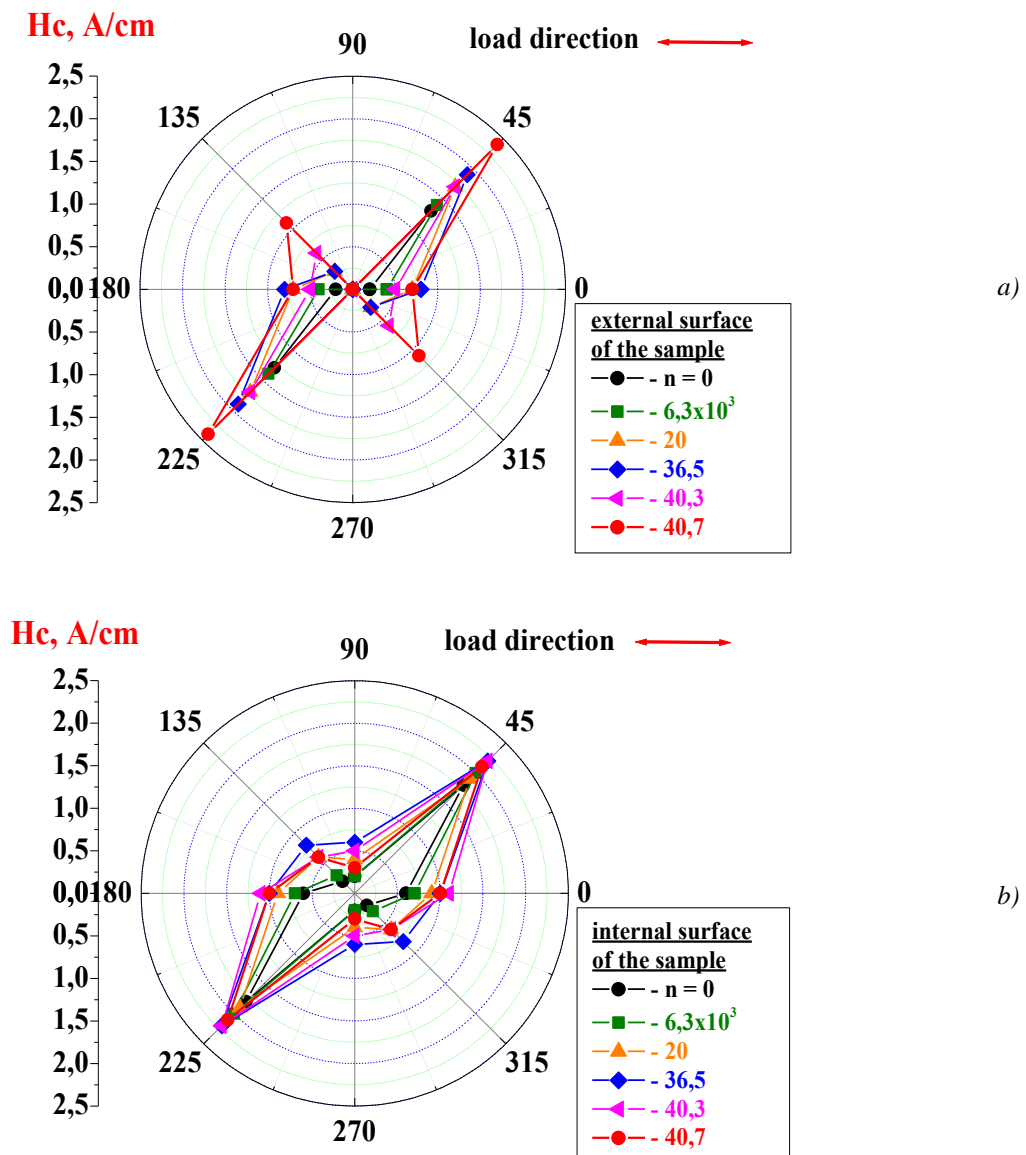


**Figure 26.** The diagrams of the coercive force values distribution from two opposite sides (respectively, (a) and (b)) of the continuous sample parts (without weld joint) between the edge of the sample working part and the weld joint

The differences in the character of the coercive force values distribution on the opposite sample surfaces outside the weld joint are due to technological damage during the pipe formation from the sheet metal with the longitudinal weld joint the laboratory samples were made of. The discrepancy of the coercive force maximum values direction with the load direction is probably caused by the effect of the residual deformations from the calibrations with the «scroll» of the pipe, since the cyclic loading was carried out under stresses equal to the

metal endurance limits when there were no significant changes in the structure that were not fixed by a structroscope.

The carried out tests on multi-cycle fatigue of laboratory samples with stress concentrators showed that when loading at stresses equal to the limits of endurance in very small metal volumes in the concentrators zone, the metal elastic-plastic deformation occurs resulting in the significant changes in the metal structure and, relatively, of the coercive force values, on the background of elastic deformation, of sufficiently large volume of the rest of the metal determined by the sensor dimensions. In this rather large volume of the remaining metal no essential structure changes and relatively coercive force place. The device sensitivity to the coercive force values change in the values in the stress concentration zones under the load is determined by the ratio of elastic and plastic deformed metal volumes in the measuring zone.

Thus, despite the small absolute values of the coercive force and the differences in their values on the opposite sample surfaces with the stress concentrators, the presence of the concentrators causes the increase in  $H_c$  values in these zones from the sample opposite sides and makes it possible to detect the surface and under surface defects.

**Generalization of the experimental investigatin results.** It follows from the obtained experimental data that for static or cyclic austenitic unstable steels including alternating one, the deformation causes structural transformations of the original austenite into the deformation martensitic with finite ferritic-perlite decay that causes the change in the metal magnetic properties during the transition from paramagnetic to ferromagnetic state and, as a consequence, corresponding coercive force changes.

Under the «soft» load, when the fracture is caused by the deformation accumulation to the critical values that correspond, approximately, to the relative metal elongation when tensile, the measured values of the coercive force can serve as a measure of the initial plasticity implementation ( $\delta$ ). At the same time, it is necessary to take into account changes in the direction of the kinetic coercive force curve under loading. The increase in the coercive force values under the load to the maximum values corresponds to the deformations accumulation, including cyclic creep and, respectively, the stage of cracks initiation (without loss of metal solidity). If under the operating conditions the product plastic deformation is permissible, then the fracture risks are minimal. Reduction of the coercive force after reaching the maximum values change in the direction of the kinetic curve  $H_c$  towards the decrease direction) characterizes the process of metal solidity in the form of pores and cracks, corresponds to the cracks initiation stage and significantly increases the fracture risk.

Under the «hard» load, when fracture occurs due to the cracks initiation and development to critical values, the cyclic load also causes the monotonous increase in the coercive force values to the maximum values, which are approximately 30% smaller than the similar values under tension, after which there is a sharp decrease in  $H_c$  values. Under cyclic loading, the growth area of the coercive force values in terms of the load cycles number corresponds to the stage of the cracks initiation and the product fracture risks are minimal. Similar to the «soft» load, the decrease in the coercive force values after reaching their maximum values characterizes the process of metal solidity loss in the form of cracks, corresponds to the stage of cracks development and significantly increases the fracture risks.

Under the operation conditions, while monitoring the coercive force values distribution on the product surface in the most loaded areas, special attention should be paid not to the maximum  $H_c$  values, which can exceed the similar data in the fracture zone, but to the change of the kinetic curve  $H_c$  direction on such areas. At the same time, in zones adjacent to the fracture zone due to elastic-plastic deformation, the coercive force values growth continues. Under the product operation conditions, the change in the direction of the kinetic coercive force curve indicates the completion of the cracks initiation stage and the beginning of the fracture stage (cracks development), which increases the fracture. In this case, it is reasonable to use other non-destructive control methods, for example, metal thickness measurement and ultrasonic control for determination of the defects (cracks) size and location in the metal volume of the fracture zone.

**Conclusions.** The experimental substantiation of the possibility of the damage degree estimation in the process of metal structures operation, including stress concentration zones, made of paramagnetic austenitic unstable steels, is a simple non-destructive method based on the results of coercive force measuring.

The device improvement made it possible according to the results of the coercive force measurements, in the metal local surface zones to determine the distribution of the damage level along the product surface and the kinetics of their accumulation in the most loaded sections of structural elements. This circumstance during the product operation enables us to estimate the damage degree (of different origin) of metal construction by simple non-destructive instrumental method by the same device.

The use of the improved structurescope provided the means of determination the damage accumulation stages during static or cyclic loading. The coercive force growth corresponds to the elastic-plastic deformation (the stage of cracks initiation), and decrease – to the metal solidity loss when pores or cracks occur (the stages of cracks development).

It is determined experimentally that under low cyclic loading, changes in the coercive force values are caused by structural transformations of the original austenite into deformation martensitic with finite ferritic-perlite decay and do not depend on the load type and the accumulated damage type. Quasistatic damages are formed as a result of plastic deformations accumulation, including cyclic creep resulting in the metal fracture during the initial plasticity ( $\delta$ ) implementation. Fatigue damages are generated without the accumulation of cyclic creep deformations and when the metal fracture is caused by the action of alternating reverse deformations resulting in the fatigue cracks initiation and development to the critical values.

Under tension or cyclic alternating deformation the residual metal strength can be estimated by the coercive force value on the ascending or descending sections of the kinetic curves  $H_c$ .

The determination of the damage accumulation stage by changing the direction of the kinetic coercive force curves after a certain number of operating time cycles makes it possible to construct the irreversible damage curve (according to French) and to evaluate the cyclic durability not on the fatigue curve (fracture) of the metal, as adopted in engineering practice, but at the cracks initiation stage which significantly reduces the fracture risk.

Physically substantiated method for endurance limit determination for austenitic unstable steel based on the defining the coercive force growth rate on short bases of cyclic

loading is proposed. By means of the coercive force growth rate we can determine the value of limited endurance limit at different service life bases.

It is shown the possibility of using the structuroscope in order to detect the most deformed zones with the determination of the main stresses direction, and metal inconsistency in the form of pores and fatigue cracks is shown. Using sensors with reduced base for the coercive force measurement, it is possible to detect both surface and sub surface defects and cracks.

The application of coercimetric control enables to estimate the level of received damages according to the results of measuring the coercive force changes in the most loaded structure sections during their operation.

Under tension or cyclic alternating deformation the growth of the coercive force is associated with elastic-plastic deformation, and the decrease in  $H_c$  values is caused by the predominance of the metal solidity loss processes over the processes of ferromagnetic phase ( $\alpha$ -Fe) formation. At the same time, changes in the metal structure, estimated by the percentage of the ferromagnetic phase ( $\alpha$ -Fe) fraction, do not reflect the damage accumulation processes.

The fixed limits in the possibility of the estimation of the metal damage degree in multi-cyclic fatigue, including stress concentration zones according to coercive force measurements caused by the device sensitivity (with the given sensor dimensions for  $H_c$  measurement) to the ratio of elastic and plastic-deformed metal volumes in the fracture zone (measurement) are determined.

The obtained results can be the basis for the development of new approaches concerning the rapid estimation of the metal constructions residual life by a simple non-destructive method.

Роботу виконано в рамках науково-дослідної роботи відділу втоми і термовтоми матеріалів Інституту проблем міцності імені Г. С. Писаренка НАН України за темою 1.3.4.1910 «Розробка методів оцінки втомного пошкодження металічних матеріалів на стадіях зародження і росту тріщин».

## References

1. Gopkalo A. P., Bezlyudko G. Ya., Nehotyashiy V. A. K ekspertnoy otsenke povrezhdennosti stali AISI 304 pri staticheskom i tsiklicheskom nagruzhении po izmereniyam koertsitivnoy silyi. V mire nerazrushayushchego kontrolya. Sankt Peterburg, 2017. Tom. 20. P. 45–51.
2. Gulyaev A. P. Metallovedenie. Moskva, 1951. 484 p.
3. Gopkalo O., Bezlyudko G., Nehotyashiy V. Otsinka poshkodzhenn metalu konstruktsiy pri statichnomu ta tsiklichnomu deformuvanni po kinetitsi koertsitivnoyi sili. Poshkodzhennya materialiv pid chas ekspluatatsiyi, metodi yogo diagnostuvannya i prognozuvannya: pratsi konferentsiyi. (Ternopil, 19–22 veresnya 2017 r.). Ternopil, 2017. P. 73–78.
4. Gopkalo O., Bezlyudko G., Nehotyashiy V. Evaluation of the structures metal damage under the static and cyclic loadings according to the coersive force value. Scientific Journal of TNTU. TNTU. 2018. Vol. 89. No. 1. P. 19–32. [https://doi.org/10.33108/visnyk\\_tntu2018.01.019](https://doi.org/10.33108/visnyk_tntu2018.01.019)

## Список використаної літератури

1. Гопкало А. П., Безлюдько Г. Я., Нехотящий В. А. К экспертной оценке поврежденности стали AISI 304 при статическом и циклическом нагружении по измерениям коэрцитивной силы. В мире неразрушающего контроля. Санкт Петербург. 2017. Том. 20. С. 45–51.
2. Гуляев А. П. Металловедение. Москва, 1951. 484 с.
3. Гопкало О., Безлюдько Г., Нехотящий В. Оцінка пошкоджень металу конструкцій при статичному та циклічному деформуванні по кінетиці коерцитивної сили. Пошкодження матеріалів під час експлуатації, методи його діагностування і прогнозування: матеріали наук.-практ. конф. (м. Тернопіль, 19–22 вересня 2017 р.). Тернопіль, 2017. С. 73–78.
4. Gopkalo O., Bezlyudko G., Nehotyashiy V. Evaluation of the structures metal damage under the static and cyclic loadings according to the coersive force value. Scientific Journal of TNTU. TNTU. 2018. Vol. 89. No. 1. P. 19–32. [https://doi.org/10.33108/visnyk\\_tntu2018.01.019](https://doi.org/10.33108/visnyk_tntu2018.01.019)



УДК 539.4

# ДО ОЦІНЮВАННЯ ПОШКОДЖЕНОСТІ ЕЛЕМЕНТІВ КОНСТРУКЦІЙ ЗА ВИМІРАМИ КОЕРЦИТИВНОЇ СИЛИ. ПОВІДОМЛЕННЯ 2. РЕЗУЛЬТАТИ ЕКСПЕРИМЕНТАЛЬНИХ ДОСЛІДЖЕНЬ ВИКОРИСТАННЯ КОЕРЦИТИМЕТРИЧНОГО КОНТРОЛЮ ДЛЯ ОЦІНЮВАННЯ СТУПЕНЯ ПОШКОДЖЕННЯ ПАРАМАГНІТНОЇ АУСТЕНІТНОЇ СТАЛІ ПРИ МЕХАНІЧНОМУ НАВАНТАЖЕННІ

Олексій Гопкало<sup>1</sup>; Володимир Нехотящий<sup>2</sup>; Геннадій Безлюдько<sup>3</sup>;  
Олена Гопкало<sup>1</sup>; Юрій Кураш<sup>1</sup>

<sup>1</sup>Інститут проблем міцності імені Г. С. Писаренка НАН України,  
Київ, Україна

<sup>2</sup>Інститут електрозварювання імені Є. О. Патона НАН України,  
Київ, Україна

<sup>3</sup>ООО «Специальные научные разработки», Харків, Україна

**Резюме.** Наведено результати експериментальних досліджень реагування коерцитивної сили на механічні навантаження лабораторних зразків із парамагнітної (у вихідному стані) нестабільної аустенітної сталі AISI 304 (08X18H9), яке пов'язано зі структурними перетвореннями вихідного аустеніту в деформаційний мартенсит з кінцевим феррито-перлітним розпадом, що викликає зміну магнітних властивостей металу з парамагнітного у феромагнітний стан. Наведено результати експериментальних досліджень реагування коерцитивної сили на відмінні за пошкоджувальною дією види навантаження: розтяг та малоциклове навантаження при контролі амплітуди напружень («м'яке» навантаження), яке зумовлює квазістатичне руйнування шляхом реалізації вихідної пластичності металу ( $\delta$ ), та малоциклове навантаження при контролі амплітуди деформації («жорстке» навантаження), яке зумовлює руйнування від втоми, внаслідок зародження та розвитку до критичних значень тріщин втоми. Представлені також результати експериментальних досліджень реагування коерцитивної сили на механічні навантаження при напруженнях, характерних для багатоциклової втоми та за наявності концентраторів напружень. За результатами випробувань встановлена стадійність процесів накопичення пошкоджень при «м'якому» та «жорсткому» навантаженнях: зростання значень коерцитивної сили відповідає пружно-пластичному деформуванню (стадії зародження тріщин), а зниження їх значень пов'язано зі втратою суцільності металу при появі пор або тріщин (стадії розвитку тріщин). Встановлення стадійності накопичення пошкоджень за зміною напрямку кінетичної кривої коерцитивної сили після певного числа циклів напруження дозволяє побудувати криву незворотної пошкоджуваності (за Френчем) і проводити оцінювання циклічної довговічності не по кривій втоми (руйнуванню) металу, як прийнято в інженерній практиці, а на стадії зародження тріщин, що істотно знижує ризики руйнування. Запропоновано фізично обґрунтований метод встановлення границі витривалості для аустенітної нестабільної сталі, який базується на визначенні швидкості зростання коерцитивної сили на коротких базах циклічного навантаження. За величиною швидкості зростання коерцитивної сили можна встановлювати значення границі витривалості на різних базах довговічності. Показана можливість використання структуроскопу для виявлення найбільш деформованих зон зі встановленням напрямку головних напружень, та несуцільності металу у вигляді пор і тріщин втоми, поверхневих та підповерхневих дефектів і тріщин. Встановлено обмеження у можливості оцінювання ступеня пошкодження металу при багатоциклової втомі, у тому числі зонах концентраторів напружень, за вимірами значень коерцитивної сили, які зумовлені чутливістю приладу до співвідношення об'ємів пружно та пластично деформованого металу в зоні руйнування (вимірювання). Використання коерцитиметричного контролю дозволяє за результатами вимірювання змін коерцитивної сили у найбільш навантажених ділянках конструкцій при їх експлуатації оцінити рівень отриманих пошкоджень.

**Ключові слова:** структуроскоп, коерцитивна сила, навантаження, пошкодження, напруження, деформація, руйнування.

[https://doi.org/10.33108/visnyk\\_tntu2019.02.007](https://doi.org/10.33108/visnyk_tntu2019.02.007)

Отримано 18.04.2019